ANTIOXIDANTS & REDOX SIGNALING
Volume 14, Number 2, 2011

DOI: 10.1089/ars.2010.3190

ORIGINAL RESEARCH COMMUNICATION

Ajoene, A Stable Garlic By-Product, Inhibits High Fat Diet-Induced Hepatic Steatosis and Oxidative Injury Through LKB1-Dependent AMPK Activation

Chang Yeob Han,[1] Sung Hwan Ki,[1] Young Woo Kim,[1] Kyoung Noh,[1] Da Yeon Lee,[2] Bomi Kang,[2] Jae-Ha Ryu,[2] Raok Jeon,[2] Eun Hyun Kim,[3] Se Jin Hwang,[3] and Sang Geon Kim[1]

Abstract

Hepatic steatosis, a hepatic component of metabolic syndrome, is common and may progress to steatohepatitis and cirrhosis. The liver X receptor-α (LXRα)-sterol regulatory element binding protein-1c (SREBP-1c) pathway plays a key role in hepatic steatosis. This study investigated the potential of ajoene, a stable garlic by-product, to inhibit high fat diet (HFD)-induced hepatic steatosis and the underlying mechanism. Ajoene treatment attenuated fat accumulation and induction of lipogenic genes in the liver of HFD-fed mice. Blood biochemical analyses and histopathologic examinations showed that ajoene prevented liver injury with the inhibition of oxidative stress, as evidenced by thiobarbituric acid reactive substances formation and nitrotyrosinylation. Moreover, ajoene treatment inhibited LXRα agonist (T0901317)-mediated SREBP-1c activation, and transactivation of the lipogenic target genes in hepatocytes. Ajoene was found to activate AMP-activated protein kinase (AMPK) via LKB1, responsible for the inhibition of p70 ribosomal S6 kinase-1 (S6K1). The ability of ajoene to repress T0901317-induced SREBP-1c expression was antagonized by inhibition of AMPK or activation of S6K1, supporting the role of these kinases in the antisteatotic effect. Our results demonstrate that ajoene has an effect of activating AMPK through LKB1 and inhibit S6K1 activity, contributing to the prevention of SREBP-1c-mediated hepatic lipogenesis via the inhibition of LXRα activity. *Antioxid Redox Signal.* 14, 187–202.

Introduction

Nonalcoholic fatty liver disease (NAFLD) is a common liver disease that refers to the range of liver damage from steatosis to nonalcoholic steatohepatitis and cirrhosis (35). Moreover, NAFLD is considered to be the major hepatic component of metabolic syndrome (25). Features of metabolic syndrome include obesity, insulin resistance, and cardiovascular diseases. In obese people, most with insulin resistance, excessive fat is accumulated in the liver and the elevated hepatic lipid content is closely associated with pathogenesis of the syndrome (25). In hepatocytes, fat amounts are enhanced by induction of lipogenesis, as well as by increased delivery of fatty acids and diminished export of triglyceride (TG), which eventually results in chronic liver diseases in conjunction with systemic metabolic dysfunction (25, 35).

Liver X receptor-α (LXRα) is a nuclear receptor that acts as a regulator to increase lipid synthesis in the liver (39). Sterol regulatory element binding protein-1c (SREBP-1c) is a target gene of LXRα, and is a key transcriptional regulator of lipogenic genes encoding enzymes to promote fat accumulation in the liver, which include fatty acid synthase (FAS), acetyl-CoA carboxylase (ACC), and stearoyl-CoA desaturase-1 (SCD-1) (33). Chemical activation of LXRα promotes SREBP-1c-dependent induction of the lipogenic genes, causing increases in fatty acid synthesis and further progression to hepatic steatosis and hypertriglyceridemia (39). Therefore, the lipogenic pathway mediated by LXRα-SREBP-1c is an attractive target for the prevention and/or treatment of hepatic steatosis and steatohepatitis.

AMP-activated protein kinase (AMPK) is an intracellular sensor for energy homeostasis (30). Diverse physiologic responses associated with lipid and glucose metabolism are mediated by the AMPK-dependent pathway. The activation of this kinase inhibits hepatic lipogenesis mainly through inhibitory phosphorylation of ACC, a rate-controlling enzyme of fatty acid synthesis. Cholesterol production is also inhibited by AMPK activation in the liver via suppression of

[1]College of Pharmacy and Research Institute of Pharmaceutical Sciences, Seoul National University, Seoul, Korea.
[2]College of Pharmacy, Sookmyung Women's University, Seoul, Korea.
[3]College of Medicine, Hanyang University, Seoul, Korea.

3-hydroxy-3-methylglutaryl-CoA reductase (48). In addition, AMPK activation reduces gluconeogenesis in liver and enhances glucose uptake in skeletal muscle (30). Activated mutant of AMPK inhibits mammalian target of rapamycin/p70 ribosomal S6 kinase-1 (S6K1) signaling cascade (20). Our previous finding indicates that AMPK activation and AMPK-dependent S6K1 inhibition contributes to antidiabetic and antisteatotic action (2, 18). Furthermore, these enzymes oppositely regulate the LXRα activity via phosphorylation at different residues, which affects LXRα-mediated steatosis in the liver (18).

Garlic (*Allium sativum*) is a widely consumed natural product and has medicinal properties. Among the constituents of garlic, ajoene (4,5,9-trithiadodeca-1,6,11-triene-9-oxide) is a biologically active organosulfur compound (19), and exerts beneficial effects such as anticancer, anti-atherosclerosis, and antimicrobial actions (1, 37, 46). Allicin also has biological actions similar to ajoene, but is highly unstable as shown by thermostability analysis (12). Ajoene is largely generated from allicin in crushed garlic by sulfoxide rearrangement in heat condition (12), and thus has chemical stability (15). Moreover, ajoene can be easily made by organic synthesis, which may offer an advantage for development of a drug candidate and clinical use. Regardless of the intensive studies of garlic products, molecular mechanisms mediated by specific garlic component(s) are poorly understood; furthermore, the effects of ajoene on lipid metabolism and its associated conditions or diseases have never been explored.

This study investigated whether ajoene inhibits high fat diet (HFD)-induced hepatic steatosis and, if so, the mechanistic basis. Our findings demonstrate that ajoene has the ability to prevent SREBP-1c-dependent lipogenesis in the liver via the inhibition of LXRα activity and thereby reverse hepatic steatosis and steatohepatitis. Moreover, we found that ajoene treatment activates AMPK via liver kinase B1 (LKB1) and inhibits S6K1 in hepatocytes, and that the beneficial antisteatotic effect of ajoene is mediated with the regulation of AMPK-S6K1 pathway, providing the possibility of a new therapeutic application of this agent for NAFLD and/or other metabolic dysfunctions.

Materials and Methods

Reagents

Antibodies directed against SREBP-1, AMPK, and LKB1 were supplied by Santa Cruz Biotechnology (Santa Cruz, CA). Antiphospho-AMPK, antiphospho-ACC, anti-ACC, antiphospho-S6, anti-S6, and antiphospho-LKB1 antibodies were obtained from Cell Signaling (Beverly, MA). Antibodies recognizing inducible nitric oxide synthase (iNOS) and cyclooxygenase-2 (COX-2) were provided from BD biosciences (San Jose, CA) and Cayman (Ann Arbor, MI), respectively. Horseradish peroxidase-conjugated goat anti-rabbit and goat anti-mouse IgGs were purchased from Zymed Laboratories (San Francisco, CA). 22(R)-Hydroxycholesterol, GW3965, diallyl sulfide (DAS), diallyl disulfide (DADS), and other reagents were supplied from Sigma-Aldrich (St. Louis, MO).

Chemical synthesis and characterization of ajoene

Ajoene was synthesized according to the modified Hunter's method (17). Allyl thiol was propargylated, followed by regioselective radical addition of thiolacetic acid, to make vinyl thioacetate. Deprotection of thioacetate with hydroxide in methanol and subsequent sulfenylation of the enethiolate with S-allyl *p*-toluenesulfonylthioate yielded vinyl disulfide. The resultant disulfide was chemoselectively oxidized by treatment of meta-chloroperoxybenzoic acid (m-CPBA) (Fig. 1A). The chemical structure of (Z)-ajoene was confirmed by mass spectrometry and NMR analyses (Figs. 1B and 1C).

Animal treatment

All animal experiments were approved by the Seoul National University Animal Experiment Ethics Committee, and were conducted in accordance with the institutional guidelines for care and use of laboratory animals. Male C57BL/6 mice were obtained from Charles River Orient (Seoul, Korea) and were acclimatized for 1 week in a clean room at the Animal Center for Pharmaceutical Research, Seoul National University. At 7 weeks of age, C57BL/6 mice were started on either a normal diet (ND) or an HFD (60% of kcal as fat, Product #D12492, Research Diets, New Brunswick, NJ) for 8 weeks: the animals were distributed into three treatment groups [i.e., HFD+vehicle, HFD+ajoene (10 mg/kg/day), and HFD+ajoene (30 mg/kg/day), $n = 8$ each] after 4 weeks of diet feeding. Then, ajoene dissolved in 40% polyethyleneglycol #400 was orally administered to mice 5 times per week during the last 4 weeks of diet feeding. Six hours after last ajoene administration, mice were fasted overnight ($\sim$16 h), and blood samples were drawn by retro-orbital puncture. The animals were sacrificed by carbon dioxide euthanasia.

Hematoxylin and eosin, and Oil Red O stainings

The left lateral lobe of the liver was sliced, and tissue slices were fixed in 10% buffered-neutral formalin for 6 h. The fixed liver tissue slices were embedded in paraffin, and cut into 4 μm thick sections, which were stained with hematoxylin and eosin (H&E) (27). Histopathology was assessed by light microscopy. A certified pathologist examined the samples in a blinded fashion. For Oil Red O (Sigma) staining, 4 μm sections were cut from frozen optimal cutting temperature samples, affixed to microscope slides, and allowed to air-dry overnight at room temperature. The liver sections were stained in fresh Oil Red O for 10 min and rinsed in water (18).

Triglyceride measurement

Samples of mouse liver (0.3 g) were homogenized in 0.1 *M* Tris–acetate buffer (pH 7.4) containing 0.1 *M* potassium chloride and 1 m*M* EDTA. Six volumes of chloroform:methanol (2:1) were then added. After vigorous stirring, the mixtures were incubated on ice for 1 h and then centrifuged at 800 *g* for 3 min. The resulting lower phase was aspirated. The TG content was determined using Sigma Diagnostic Triglyceride Reagents (18).

Blood chemistry

Plasma alanine aminotransferase (ALT), TG, and total cholesterol were analyzed using Spectrum®, an automatic blood chemistry analyzer (Abbott Laboratories, Abbott Park, IL). Fasting glucose in plasma was measured using Accu-Chek Active (Roche, Germany).

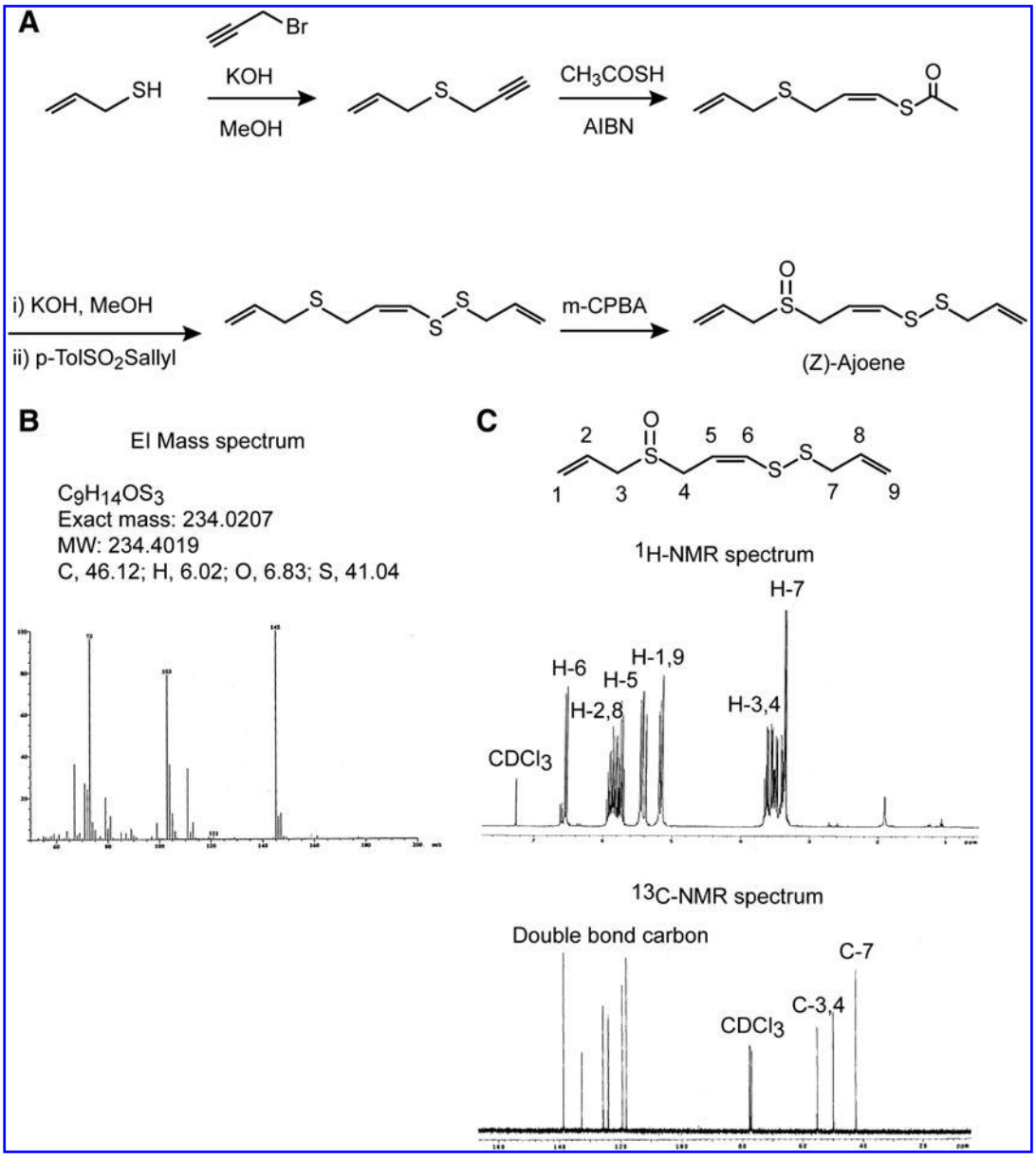

FIG. 1. Chemical synthesis and characterization of ajoene. (**A**) The synthetic pathway of (Z)-ajoene. (Z)-Ajoene was synthesized as described in the Materials and Methods section. (**B**) Electron impact (EI) mass spectrum. (**C**) NMR analyses. Hydrogen-1 NMR (*upper*) and carbon-13 NMR (*lower*).

Thiobarbituric acid reactive substances assay

Thiobarbituric acid reactive substances (TBARS) formation was determined in liver homogenates, and the amounts were referenced as moles of malonyldialdehyde (MDA) using an MDA standard (4). Briefly, MDA-thiobarbituric acid adduct was formed by the reaction of MDA present in the sample and thiobarbituric acid solution under high temperature (90°–100°C) and acidic conditions. The absorbance was measured at 532 nm.

Immunohistochemistry

Liver specimens were fixed in 10% formalin, embedded in paraffin, cut into 4-μm-thick sections, and mounted on slides. Tissue sections were immunostained with antibodies directed against nitrotyrosine (Millipore, Billerica, MA). Briefly, tissue sections were deparaffinized and were incubated with rabbit anti-nitrotyrosine (1:200) for 16 h, followed by incubation with Cy3-conjugated donkey anti-rabbit antibody for 2 h (27).

Determination of reduced glutathione

Reduced glutathione (GSH) in the liver tissue was quantified using a commercially available GSH determination kit (Oxis International, Portland, OR). Briefly, the GSH-400 method was based on a chemical reaction which proceeded in two steps. The first step led to the formation of substitution products (thioethers) between 4-chloro-1-methyl-7-trifluromethyl-quinolinum methylsulfate and all mercaptans present in the samples. The second step included β-elimination reaction

under an alkaline condition. This reaction was mediated by 30% NaOH which specifically transformed the substituted product (GSH-thioether) into a chromophoric thione.

Determination of glutathione peroxidase and catalase activities

The activities of glutathione peroxidase (GPx) and catalase were quantified using commercially available systems, GPx (Cayman, Ann Arbor, MI) and catalase assay kits (Sigma-Aldrich), respectively. Briefly, GPx activity was measured by a coupled reaction with glutathione reductase. Oxidized GSH (GSSG), produced upon reduction of hydroperoxide by GPx, was recycled to its reduced state by glutathione reductase and NADPH (36). The oxidation of NADPH to $NADP^+$ was accompanied by a decrease in absorbance at 340 nm. Catalase activity was determined by measuring hydrogen peroxide substrate remaining after the action of catalase. First, catalase converted hydrogen peroxide to water and oxygen, which was stopped with sodium azide. An aliquot of the reaction mixture was colorimetrically assayed using a substituted phenol (3,5-dichloro-2-hydroxybenzene-sulfonic acid), which coupled to 4-aminoantipyrine in the presence of hydrogen peroxide and horseradish peroxidase to yield a red quinoneimine dye (N-(4-antipyryl)-3-chloro-5-sulfonate-p-benzoquinone-monoimine) (absorbance at 520 nm).

Cell culture and in vitro *assays*

HepG2 cells, a human hepatocyte-derived cell line, were purchased from ATCC (Rockville, MD). Primary hepatocytes were isolated from male Sprague-Dawley rats (23). Cells were plated at 1×10^5 per well in 6-well plates, and wells with 70%–80% confluency were used. All cells were maintained in Dulbecco's modified Eagle's medium containing 10% fetal bovine serum, 50 units/ml penicillin and 50 μg/ml streptomycin at 37°C in humidified atmosphere with 5% CO_2. The cells were treated with vehicle or LXR agonist [i.e., T0901317, 10 μM GW3965, and 10 μM 22(R)-hydroxycholesterol] in the presence or absence of ajoene for 12 h. In addition, the effect of 30 μM DAS or DADS on ACC phosphorylation was compared with that of ajoene.

RNA isolation and real-time PCR assays

Total RNA was extracted using Trizol (Invitrogen, Carlsbad, CA) according to the manufacturer's instructions. Total RNA (1 μg) was reverse-transcribed using an oligo$(dT)_{16}$ primer to obtain cDNA. The cDNA was amplified by polymerase chain reaction (PCR). Real-time PCR was performed with a Light Cycler 1.5 apparatus (Roche, Mannheim, Germany) using a Light Cycler DNA master SYBR green-I kit according to the manufacturer's instructions. The levels of target mRNAs were normalized to those of glyceraldehyde-3-phosphate dehydrogenase (GAPDH) mRNA. The following primer sequences were used: human SREBP-1c, 5′-CGA CATCGAAGACATGCTTCAG-3′ (sense) and 5′-GGAAGGC TTCAAGAGAGGAGC-3′ (antisense); human LXRα, 5′-GAT CGAGGTGATGCTTCTGGAG-3′ (sense) and 5′-CCCTGCTT TGGCAAAGTCTTC-3′ (antisense); human FAS, 5′-GACATC GTCCATTCGTTTGTG-3′ (sense) and 5′-CGGATCACCTTCT TGAGCTCC-3′ (antisense); human ACC1, 5′-GCTGCTCG GATCACTAGTGAA-3′ (sense) and 5′-TTCTGCTATCAGT CTGTCCAG-3′ (antisense); human SCD-1, 5′-CCTCTA CTTGGAAGACGACATTCGC-3′ (sense) and 5′-GCAGCC GAGCTTTGTAAGAGCGGT-3′ (antisense); human GAPDH, 5′-GAAGATGGTGATGGGATTTC-3′ (sense) and 5′-GAAG GTGAAGGTCGGAGTC-3′ (antisense); mouse LXRα, 5′-TGCCATCAGCATCTTCTCTG-3′ (sense) and 5′-GGCTCAC CAGCTTCATTAGC-3′ (antisense); mouse SREBP-1c, 5′-AAC GTCACTTCCAGCTAGAC-3′ (sense) and 5′-CCACTAAGG TGCCTACAGAGC-3′ (antisense); mouse FAS, 5′-AGCGGC CATTTCCATTGCCC-3′ (sense) and 5′-CCATGCCCAGAG GGTGGTTG-3′ (antisense); mouse ACC1, 5′-GTCAGCGGA TGGGCGGAATG-3′ (sense) and 5′-CGCCGGATGCCATG CTCAAC-3′ (antisense); mouse SCD-1, 5′-CCGGAGACC CTTAGATCGA-3′ (sense) and 5′-TAGCCTGTAAAAGAT TTCTGCAAACC-3′ (antisense); mouse carnitine palmitoyl transferase-1 (CPT-1), 5′-GTCGCTTCTTCAAGGTCTGG-3′ (sense) and 5′-TTCTTTCGTCGTGCAAGCTA-3′ (antisense); mouse peroxisome proliferator-activated receptor γ coactivator-1α (PGC-1α), 5′-ACGAGGCCAGTCCTTCCTCC-3′ (sense) and 5′-AGCTCTGAGCAGGGACGTCT-3′ (antisense); mouse tumor necrosis factor-α (TNFα), 5′-TCCCAGGTT CTCTTCAAGGGA-3′ (sense) and 5′-GGTGAGGAGCACG TAGTCGG-3′ (antisense); and mouse GAPDH, 5′-AACGACC CCTTCATTGAC-3′ (sense) and 5′-TCCACGACATACTCAG CAC-3′ (antisense).

Transient transfection and reporter gene assays

The cells were transiently transfected with pGL2-FAS (1 μg) or TK-CYP7A1-LXREx3-LUC (0.5 μg) for 3 h in the presence of Lipofectamine® (Invitrogen, Carlsbad, CA) reagent. The activity of luciferase was measured by adding luciferase assay reagent (Promega, Madison, WI). The FAS reporter plasmid (pGL2-FAS) was a gift from Dr. T. F. Osborne (University of California, Irvine, CA). Dr. D. J. Mangelsdorf (Howard Hughes Medical Institute, University of Texas Southwestern Medical Center, Dallas, TX) provided the luciferase reporter plasmid TK-CYP7a-LXRE(X3)-LUC that contains three tandem copies of the sequence (5′-gcttTGGTCActcaAGTTCAagtta-3′) from the rat CYP7A1 gene.

Chromatin immunoprecipitation assay

The cells were treated with T090 or T090+ajoene for 6 h following dominant negative (DN)-AMPK transfection, and then formaldehyde was added to the cells to a final concentration of 1% for cross-linking of chromatin. The chromatin immunoprecipitation assay was performed according to the chromatin immunoprecipitation (ChIP) assay kit protocol (Upstate Biotechnology, Lake Placid, NY). PCR was performed using the specific primer flanking the LXRE region of the SREBP-1c gene promoter (sense, 5′-TCAGGGTGCCAGCGAACC-3′, and antisense, 5′-GCTCGAGTTTCACCCCGC-3′, 207 bp).

Immunoblot analysis

Total cell lysates were prepared as previously described (18). Briefly, the cells were centrifuged at 3000 *g* for 3 min and allowed to expand osmotically to the point of lysis after the addition of lysis buffer. Lysates were centrifuged at 10,000 *g* for 10 min to obtain supernatants and were stored at -70°C until use. Immunoblot analysis was performed according to

previously published procedures (18). Protein bands of interest were developed using an ECL chemiluminescence system (Amersham, Buckinghamshire, UK). Equal protein loading was verified by immunoblotting for actin.

Data analysis

One-way analyses of variance procedures were used to assess significant differences among treatment groups. For each significant treatment effect, the Newman–Keuls test was utilized to compare multiple group means. All statistical analyses were performed using SPSS for Windows (version 15.0; SPSS, Chicago, IL). The criterion for statistical significance was set at $p < 0.05$ or 0.01.

Results

Inhibition of HFD-induced hepatic steatosis

To investigate an inhibitory effect of ajoene on fatty liver *in vivo*, mice fed an HFD (60% fat) were treated with vehicle or ajoene. Body weight gain was noticeably increased in mice fed an HFD for 8 weeks (Fig. 2A). Treatment of mice with 30 mg/kg ajoene per day for the final 4 weeks during 8 weeks of HFD feeding significantly reduced the rate of body weight gain. However, treatment of ajoene did not change the amounts of food intake (Fig. 2B). In addition, ajoene treatment at the dose of 30 mg/kg/day significantly inhibited the ability of HFD to increase the liver weight (Fig. 2C).

Since fat accumulation in the liver is the main histological feature of NAFLD, hepatic lipid accumulation was measured in the mice. As shown in Figure 2D, Oil red O staining confirmed the remarkable increase in hepatic fat in mice fed an HFD for 8 weeks, which was notably diminished by treatment of ajoene. The content of hepatic TG, the most abundant lipid accumulated in hepatocytes in NAFLD, also successfully increased in the liver of mice fed an HFD. The accumulation of hepatic TG was significantly decreased by ajoene treatment at the daily dose of either 10 mg/kg or 30 mg/kg (Fig. 2D).

Protection of HFD-induced liver injury

Because excessive fat accumulation in the liver leads to hepatitis, we determined the effect of ajoene treatment on HFD-induced liver injury. The blood biochemical analysis showed that ALT activity in plasma was increased in HFD-fed mice, which was prevented by treatment with ajoene at the dose of 30 mg/kg/day for the final 4 weeks (Fig. 3A). Consistently, HFD feeding for 8 weeks resulted in the formation of large cytoplasmic lipid droplets, hepatocyte death, and infiltration of inflammatory cells in the liver, as assessed by histopathologic examinations (Fig. 3B). Numerous vacuoles and degeneration of the hepatocytes were observed in the pericentral and intermediate zones of the liver in HFD-fed mice. The inclusion of lipid droplets and eosinophilic degeneration were markedly reduced by a low dose (10 mg/kg/day) of ajoene treatment. In particular, hepatocytes were intact in all areas and virtually no vacuolar abnormality was observed in the liver tissue of HFD-fed mice treated with 30 mg/kg/day of ajoene (Fig. 3B). In addition, the levels of inflammatory gene products were examined in the liver samples. TNFα mRNA level was increased in HFD-fed mice, which was inhibited by ajoene treatment (Fig. 3C). HFD feeding also induced iNOS and COX-2 in the liver of HFD-fed mice, which was reversed by ajoene treatment (Fig. 3D). Overall, our results demonstrate that ajoene has the effect to attenuate hepatic steatosis and protect the liver from injury in the progression of steatosis to steatohepatitis.

Inhibition of HFD-induced oxidative stress

To test whether ajoene has a protective effect on HFD-induced oxidative stress, formation of hepatic TBARS, an index of lipid peroxidation, was examined. As expected, HFD feeding increased TBARS formation in the liver tissue, which was inhibited by ajoene treatment (Fig. 4A). Moreover, the beneficial effect of ajoene on HFD-induced free radical stress was confirmed by immunohistochemical analyses for nitrotyrosine, a representative marker of protein oxidation mediated by reactive nitrogen species (RNS) (44). The intensity of nitrotyrosinylation increased in the liver tissue of mice fed an HFD, which was more severe around the pericentral area (Fig. 4B). Apparently, ajoene treatment inhibited oxidative stress-induced pathologic alteration. As expected, HFD feeding caused a decrease in hepatic GSH content, which was also antagonized by ajoene treatment (Fig. 4C). Oxidative injury may result from a decrease in the capacity of cellular antioxidant enzymes. Ajoene treatment prevented the ability of HFD-feeding to diminish GPx and catalase activities (Fig. 4D). These results show that fat accumulation causes oxidative stress and increases hepatocyte injury (i.e., TBARS formation and protein nitration in the liver), and which was inhibited by ajoene as a result of the increase in antioxidant capacity.

Inhibition of lipogenic gene induction

Given the role of LXRα-SREBP-1c pathway in hepatic fat accumulation, we examined the effects of ajoene on the expression of these genes in the liver of mice fed an HFD. The increases in mRNA levels of LXRα and SREBP-1c were observed in the HFD-fed mice, whereas treatment with ajoene inhibited HFD feeding-induced LXRα and SREBP-1c gene induction, as assessed by quantitative real-time PCR assays (Fig. 5A). Consistently, the induction of downstream lipogenic genes including FAS, ACC, and SCD-1 was decreased by ajoene treatment (Fig. 5B), indicating that repression of the LXRα-mediated lipogenic process contributes to ajoene's inhibition of hepatic fat accumulation.

In addition, the levels of TG and total cholesterol in plasma were diminished by ajoene in mice fed an HFD (Fig. 5C), being consistent with its inhibition of liver TG accumulation and lipogenic gene induction. Insulin resistance is often accompanied by the condition of fatty liver; it also occurs in an animal model fed on an HFD (51). In addition to the decrease in hepatic fat accumulation, ajoene treatment decreased HFD-induced fasting glucose and insulin contents in plasma (Fig. 4D). Taken together, our results demonstrate that ajoene has the effect to inhibit hepatic steatosis as a consequence of the inhibition of lipogenic gene induction, and that this antisteatotic efficacy is accompanied by the improvement in glucose metabolism.

Inhibition of T090-induced LXRα-SREBP-1c activation

To verify the inhibitory action of ajoene on LXRα-dependent SREBP-1c activation, the effect of ajoene on the activation of

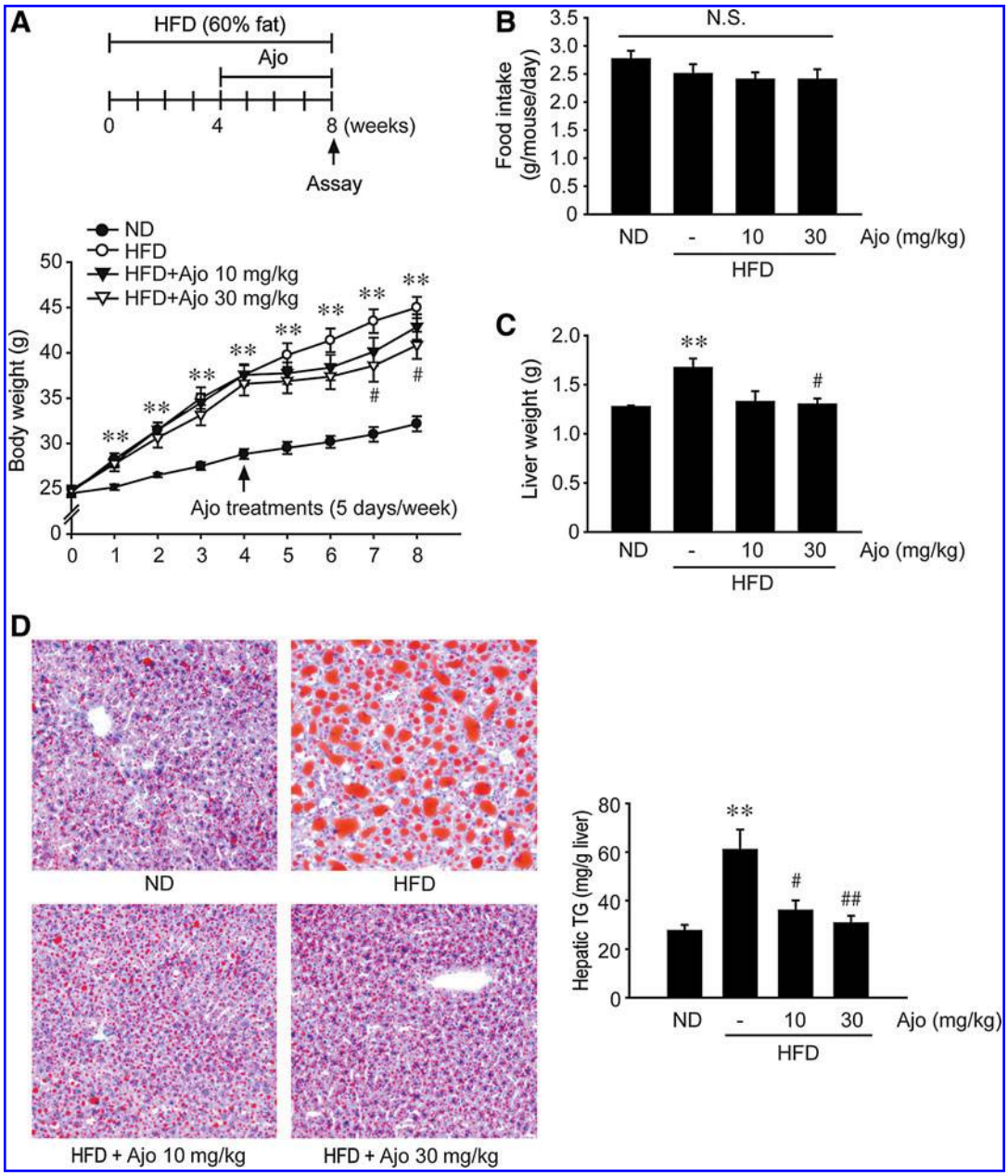

FIG. 2. Antisteatotic effect of ajoene in mice. (**A**) The effect of ajoene on body weight gain in mice. Male C57BL/6 mice were fed on either a normal diet (ND) or high-fat diet (HFD) for 8 weeks. During the final 4 weeks of diet feeding, ajoene (10 or 30 mg/kg/day) was orally administered to mice 5 times per week ($n = 8$ animals per each treatment group). (**B**) Food intake. (**C**) Changes in the liver weight. (**D**) Antisteatotic effect of ajoene. The extent of hepatic TG accumulation was assessed in HFD-fed mice treated with either vehicle or ajoene. The *left panel* shows Oil Red O staining of the liver (100X). Statistical significance of differences between each treatment group and ND ($^{**}p < 0.01$) or HFD alone ($^{\#}p < 0.05$, $^{\#\#}p < 0.01$) was determined. Ajo, ajoene; N.S., not significant. (For interpretation of the references to color in this figure legend, the reader is referred to the web version of this article at www.liebertonline.com/ars).

LXRα by T0901317 (T090, an LXRα agonist) was examined in an *in vitro* cell model. Since the promoter region of LXRα gene contains an LXR response element (LXRE), LXRα is induced by its own regulatory induction mechanism (29). In subsequent experiments, the expression of LXRα gene was monitored using real-time PCR assay in HepG2 cells. As expected, the LXRα mRNA level was increased by treatment with T090 for 12 h, whereas this effect was significantly abrogated by simultaneous ajoene treatment at either 10 μM or 30 μM concentration (Fig. 6A, left). Next, we determined whether ajoene treatment represses transactivation of the LXRα gene. The activity of CYP7A1-LXRE-luciferase (CYP7A1) gene was enhanced by treatment of the cells with T090, which was prevented by ajoene treatment (Fig. 6A, right).

Since LXRα is critical for SREBP-1c induction and the deleterious effects of LXRα activation mainly result from the increase in SREBP-1c in hepatocytes, the effect of ajoene on T090-mediated SREBP-1c expression was also measured. The level of SREBP-1c protein was induced by T090 treatment for 12 h in both HepG2 cells and primary rat hepatocytes (Fig.

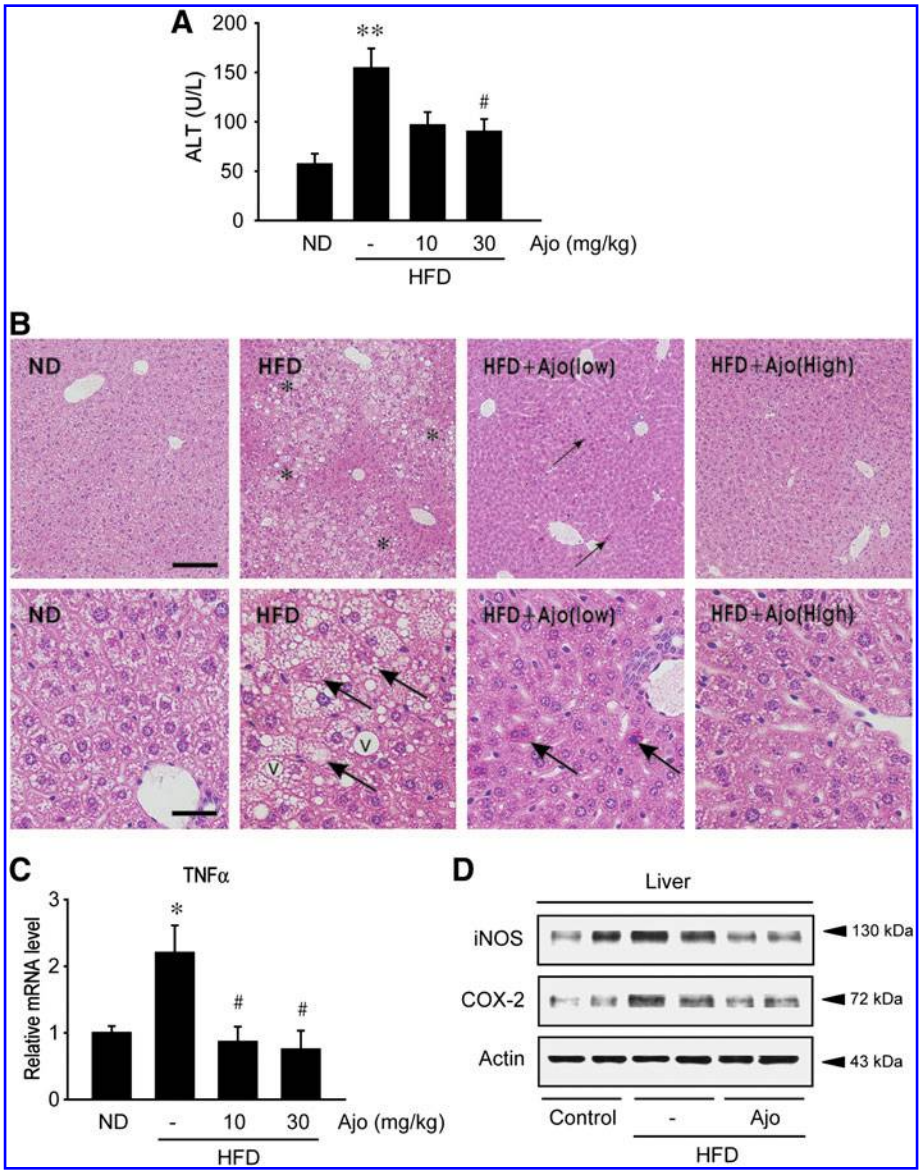

FIG. 3. Inhibition of HFD-induced liver injury. (**A**) Plasma ALT activity. (**B**) H&E staining in the liver of ND-fed mice (ND) or HFD-fed mice (HFD) treated with vehicle or 10 mg/kg/day (*Low*) or 30 mg/kg/day (*High*) ajoene. *Asterisks* indicate the formation of large cytoplasmic lipid droplets and degeneration of the hepatocytes. *Arrows* show vacuolar degeneration and necrosis of hepatocytes. V, large vacuoles. Scale bar, 100 μm (*low magnification, upper panel*) or 25 μm (*high magnification, lower panel*). (**C**) Real-time PCR assays for TNFα mRNA. The mRNA level of GAPDH was used as a reference for data normalization. (**D**) Immunoblottings for iNOS and COX-2. iNOS and COX-2 were immunoblotted in the liver homogenates of ND-fed or HFD-fed mice that had been treated with vehicle or 30 mg/kg/day ajoene. The statistical significance of differences between each treatment group and ND ($^{*}p < 0.05$, $^{**}p < 0.01$) or HFD alone ($^{\#}p < 0.05$) was determined. (For interpretation of the references to color in this figure legend, the reader is referred to the web version of this article at www.liebertonline.com/ars).

6B). The increase in SREBP-1c protein level by T090 was notably antagonized by ajoene treatment. Consistently, treatment of ajoene decreased the T090-induced SREBP-1c mRNA level (Fig. 6C). Moreover, the activities of other LXR agonists, 22(R)-hydroxycholesterol as an endogenous ligand and GW3965 as an LXR-specific agonist, to induce SREBP-1c expression were also blocked by ajoene treatment (Fig. 6D).

Repression of SREBP-1c target gene induction

SREBP-1c induces the transcription of genes encoding for lipogenic enzymes. Next, we examined whether the inhibition of SREBP-1c expression by ajoene causes the reduction of SREBP-1c activity to transactivate the target lipogenic genes. Ajoene treatment attenuated the ability of the LXRα agonist to induce the activity of FAS reporter gene containing the sterol response element (SRE) in the −150 bp FAS promoter region (Fig. 7A).Consistently, the T090-induced expression of lipogenic genes, including FAS, ACC, and SCD-1, was significantly repressed by simultaneous treatment of ajoene (Fig. 7B). These data show that the inhibition of LXRα-SREBP-1c activity by ajoene contributes to the prevention of downstream lipogenic gene induction in hepatocytes.

Activation of AMPK that leads to S6K1 inhibition

In view of the inhibitory role of AMPK activation in LXRα activity and the resultant antisteatotic effects (18), the effect of ajoene on AMPK activity was determined. The activity of AMPK was assessed by monitoring the phosphorylation of AMPKα and its best-characterized downstream kinase, ACC (30). In HepG2 cells, the levels of phospho-AMPKα and phospho-ACC were both notably increased by ajoene treatment in a time-dependent manner (Fig. 8A, left).These increases began from 10 min after ajoene treatment and were maintained at least up to 3 h. Treatment with ajoene enhanced the phosphorylations of AMPKα and ACC in a concentration-dependent manner (Fig. 8A, right). Because AMPK can inhibit the action of S6K1 that activates LXRα activity (18), the effect of ajoene on S6K1 activity was additionally examined. As expected, ajoene treatment caused commensurate decreases in the phosphorylation of S6, a substrate of S6K1 (Fig. 8A).

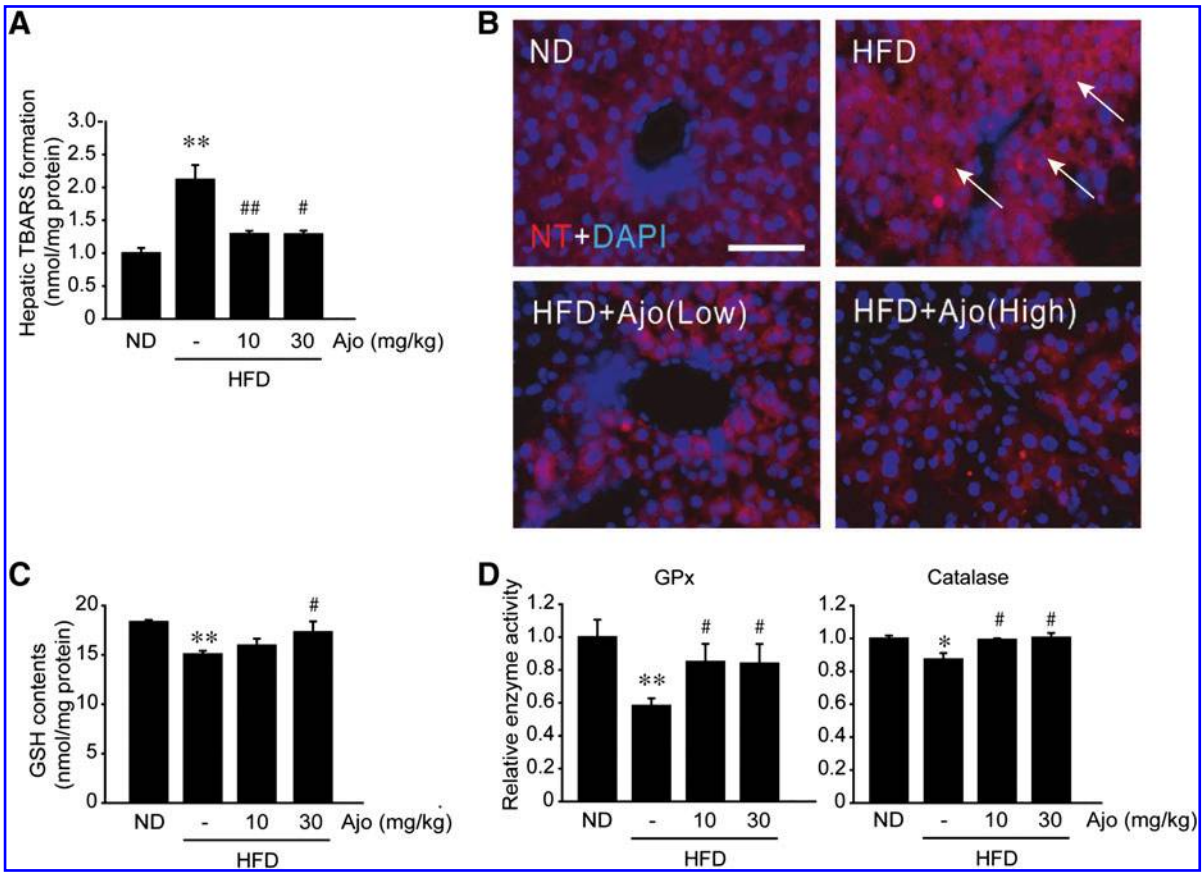

FIG. 4. Liver protection by ajoene from HFD-induced oxidative stress. (**A**) Thiobarbituric acid reactive substances (TBARS) assay. The amounts of TBARS were measured in liver homogenates. (**B**) Immunofluorescence for nitrotyrosine (*red*) in the liver of ND-fed mice (ND) or HFD-fed mice (HFD) treated with vehicle or 10 mg/kg/day (*Low*) or 30 mg/kg/day (*High*) ajoene. *Arrows* indicate the strong intensity of nitrotyrosine. Tissue sections were mounted with Vectashield containing 4′-6-diamidino-2-phenylindole (DAPI) (*blue*) for nuclear staining. Pictures are representative results from at least eight experiments. Scale bar, 50 μm. Ajo, ajoene; NT, nitrotyrosine. (**C**) Hepatic GSH content. The content of GSH was measured in liver homogenates. (**D**) Hepatic GPx and catalase activities. The enzyme activities were measured in liver homogenates. Statistical significance of differences between each treatment group and ND ($^{*}p < 0.05$, $^{**}p < 0.01$) or HFD alone ($^{\#}p < 0.05$, $^{\#\#}p < 0.01$) was determined. (For interpretation of the references to color in this figure legend, the reader is referred to the web version of this article at www.liebertonline.com/ars).

These time-dependent decreases reciprocally correlated with ACC phosphorylation that depends on AMPK activation. S6 phosphorylation then returned towards the basal level at 3 h and 6 h. DAS and DADS, which can be made from allicin, have anticancer and cholesterol-lowering properties (19). We comparatively evaluated the effects of the organosulfur compounds on AMPK activation. Treatment of cells with either 30 μM DAS or DADS only slightly increased ACC phosphorylation (Fig. 8B), indicating that these agents are less efficacious than ajoene.

To clarify whether repression of LXRα-SREBP-1c induction by ajoene results from AMPK activation and S6K1 inhibition, the effects of DN-AMPKα or constitutively active (CA)-S6K1 transfection on SREBP-1c expression were examined. In HepG2 cells, either DN-AMPKα or CA-S6K1 antagonized the ability of ajoene to inhibit T090-induced SREBP-1c expression (Fig. 8C). Consistently, ajoene treatment suppressed T090-induced LXRα binding to the LXRE region of the SREBP-1c promoter, and which was reversed by AMPK inhibition (Fig. 8D). Moreover, ajoene prevented the repression in hepatic ACC and AMPK phosphorylations elicited by HFD-feeding (Fig. 8E). It also inhibited the increased phosphorylation of S6. Our results support the roles of AMPK activation and S6K1 inhibition by ajoene in the antisteatotic effect both *in vitro* and *in vivo*. Collectively, ajoene has the capability to inhibit hepatic steatosis and protect the liver from oxidative injury, which may result from the inhibition of LXRα-mediated lipogenesis via AMPK activation that leads to S6K1 inhibition.

LKB1-dependent AMPK activation by ajoene

AMPK may be activated by LKB1 or calcium/calmodulin-dependent kinase kinase (CaMKK) through phosphorylation (30). LKB1 phosphorylation was enhanced by ajoene treatment in a time-dependent manner (Fig. 9A),which paralleled AMPK activation. Consistently, ajoene did not increase phosphorylations of ACC and AMPKα in HeLa cells deficient in LKB1 (Fig. 9B), confirming the role of LKB1 in the activation of AMPK by ajoene. Similar results were obtained by siRNA knockdown of LKB1 in HepG2 cells (Fig. 9C). AMPK activation by ajoene was unchanged by treatment with STO-609, a CaMKKβ inhibitor (Fig. 9D), suggesting that CaMKKβ is not

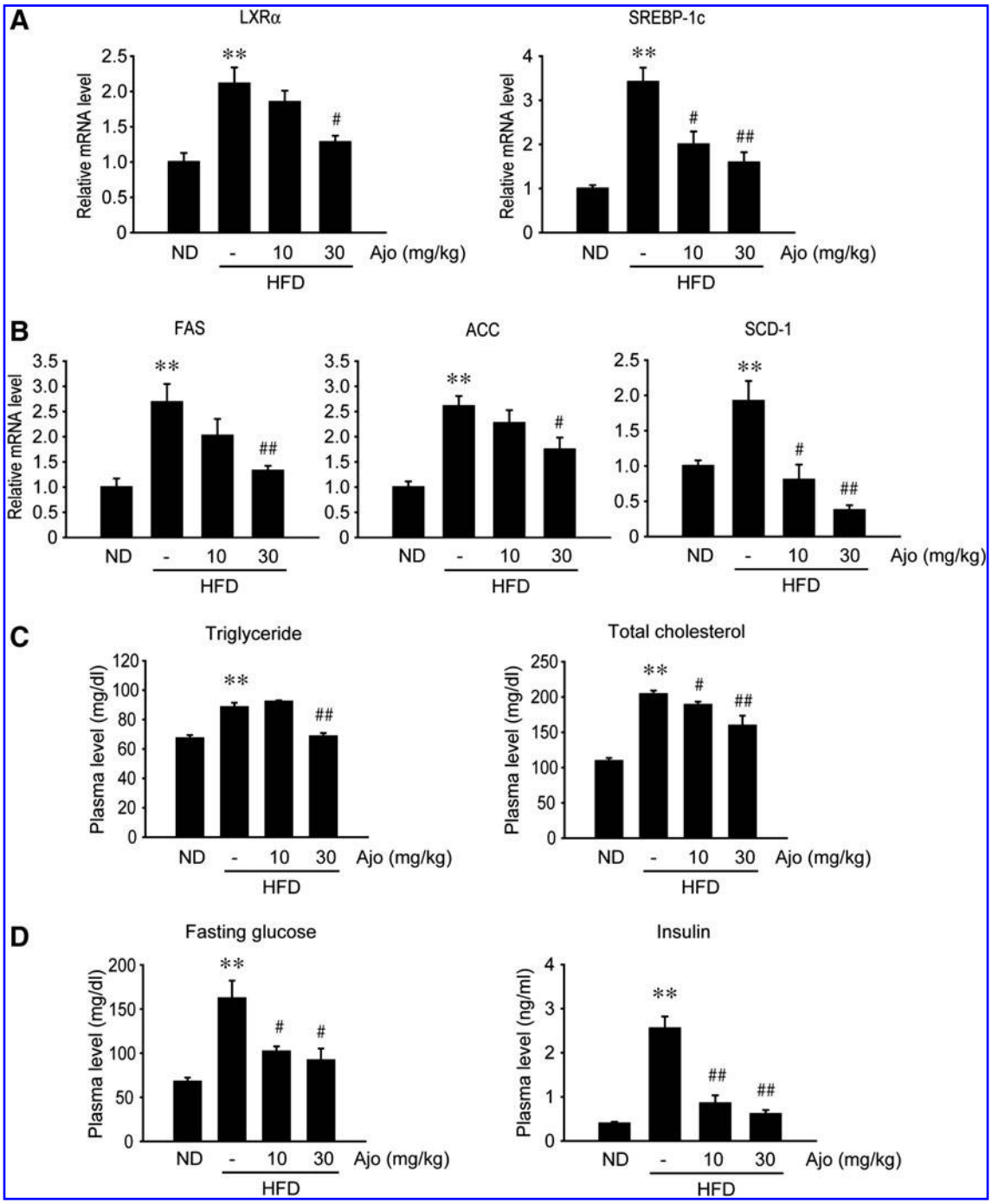

FIG. 5. Repression of hepatic lipogenic gene expression. (**A**) Real-time PCR assays for LXRα and SREBP-1c. (**B**) Real-time PCR assays for FAS, ACC, and SCD-1. The mRNA level of GAPDH was used as a reference for data normalization. (**C**) Plasma TG and total cholesterol contents. (**D**) Plasma fasting glucose level. Animals were treated as described in the legend to Figure 2A. Statistical significance of differences between each treatment group and ND (**$p < 0.01$) or HFD alone ($^{\#}p < 0.05$, $^{\#\#}p < 0.01$) was determined. Ajo, ajoene.

involved in the process. Silent information regulator T1 (SIRT1) may affect AMPK activity. In an additional experiment, ajoene treatment (30 min) increased the ratio of NAD^+/NADH in HepG2 cells (Fig. 9E). Moreover, ajoene-induced ACC and AMPKα phosphorylations were both abolished by treatment of 10 m*M* nicotinamide or 10 μM sirtinol (i.e., SIRT1 inhibitors), suggesting that SIRT1 may be required for the LKB1-dependent AMPK activation. In addition, ajoene did not change cellular ATP level. These results demonstrate that AMPK activation by ajoene may depend on the activation of LKB1 and SIRT1.

Discussion

Hepatic steatosis is emerging as the most common pathologic state of liver with the growing incidence of overweight

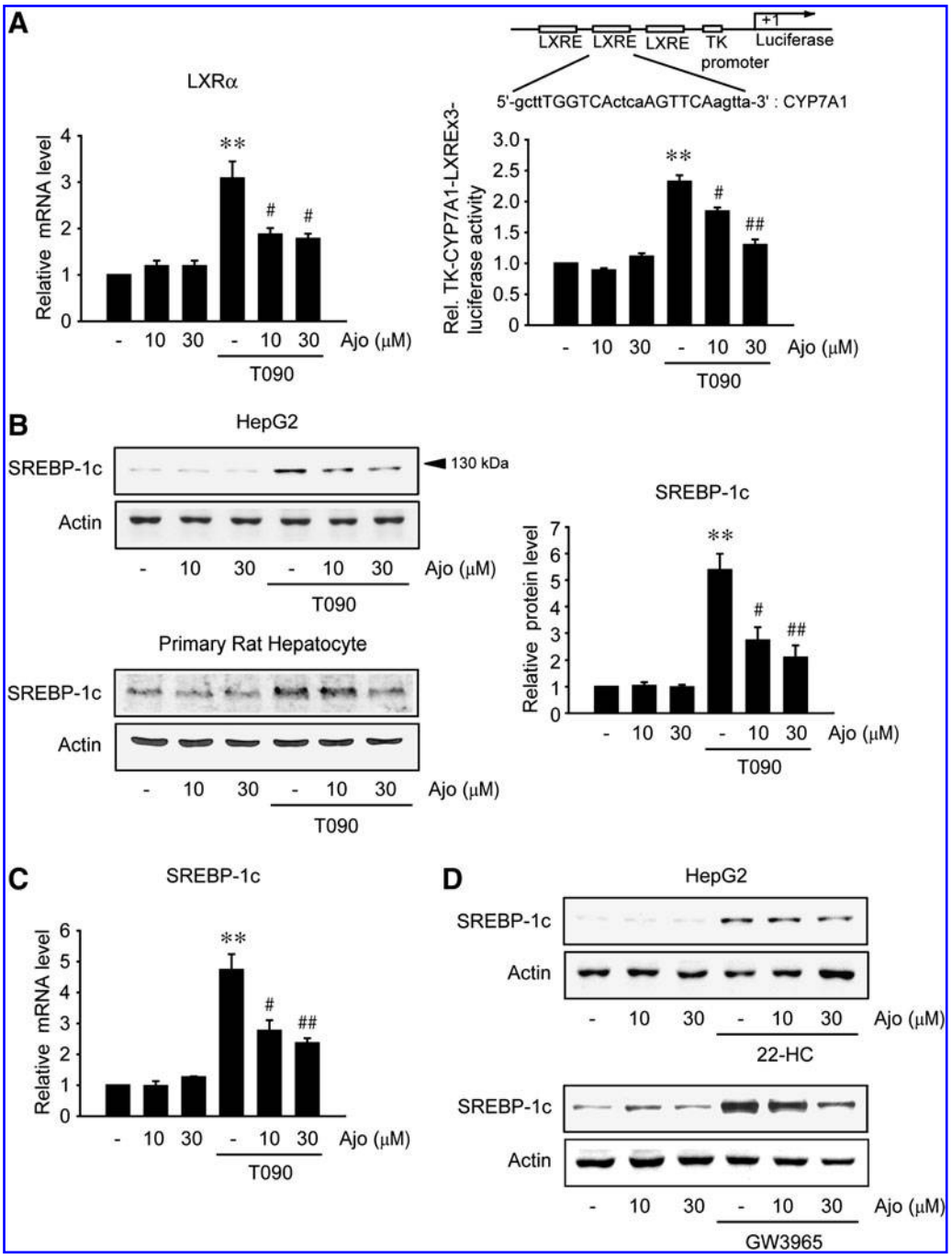

FIG. 6. The effect of ajoene on LXRα-SREBP-1c activation in hepatocytes. (**A**) Ajoene inhibition of LXRα activation. HepG2 cells were treated with vehicle or 10 μM T0901317 (T090) in combination with ajoene for 12 h. The LXRα mRNA level was analyzed using real-time RT-PCR assay (*left*), with that of GAPDH used as a normalizing reference. The relative LXRE luciferase activity (*right*) was monitored in the lysates of cells exposed to different treatment combinations (T090 for 12 h with or without ajoene pretreatment for 1 h). (**B**) The expression of SREBP-1c protein. Immunoblots were performed on the lysates of HepG2 cells or primary rat hepatocytes that had been treated with ajoene (10 μM or 30 μM) for 1 h followed by subsequent incubation with T090 for 12 h. Immunoblots are representative results from at least 3 experiments. (**C**) Real-time RT-PCR assays for SREBP-1c in HepG2 cells. (**D**) The effects of ajoene on SREBP-1c induction by 22(R)-hydroxycholesterol [22(R)-HC, 10 μM] or GW3965 (10 μM) treatment for 12 h. Data represent the mean ± S.E. of three replicates. Statistical significance of differences between each treatment group and the control ($^{**}p < 0.01$) or T090 without ajoene treatment ($^{\#}p < 0.05$, $^{\#\#}p < 0.01$) was determined. Ajo, ajoene.

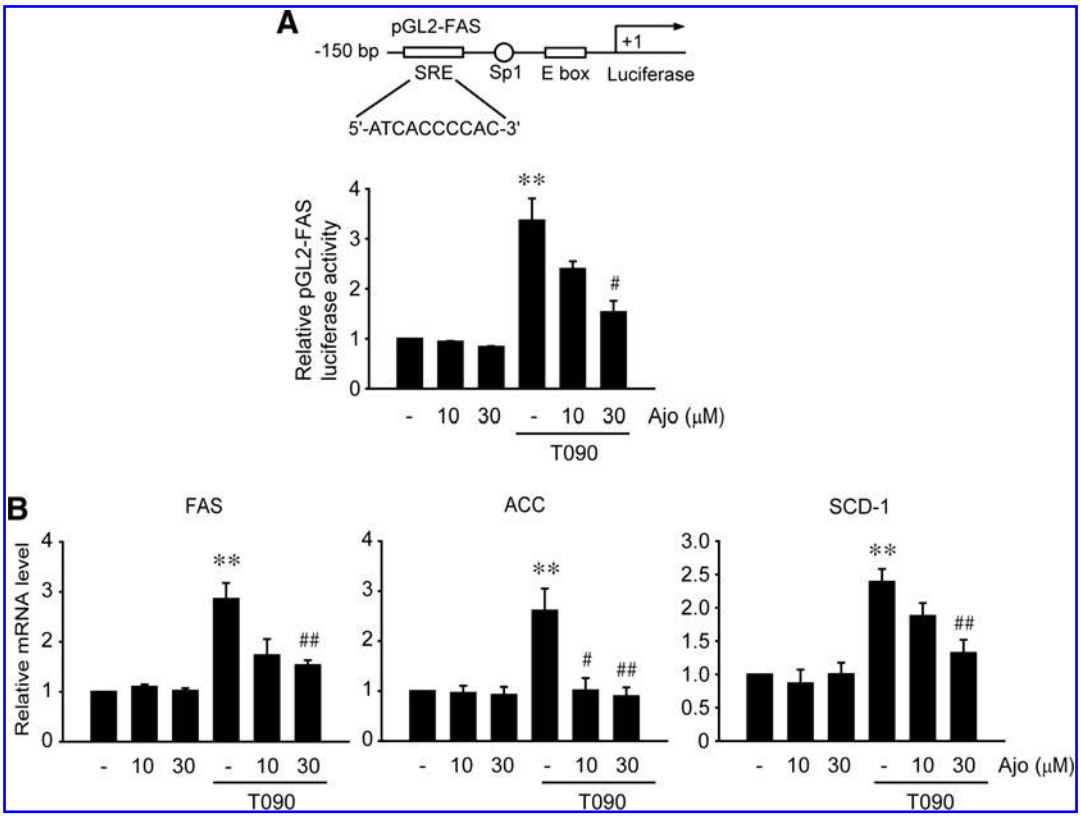

FIG. 7. Inhibition by ajoene of SREBP-1c-dependent gene induction. (**A**) Ajoene inhibition of T090-induced, SRE-mediated FAS gene transactivation. FAS luciferase assays were performed on the lysates of HepG2 cells that had been treated as described in the legend to Figure 6A. (**B**) Real-time PCR assays. HepG2 cells were treated with vehicle or T090 in combination with ajoene for 12 h. The transcripts of lipogenic genes were analyzed as described in the legend to Figure 6A. The GAPDH mRNA level was used as a normalizing reference. Data represent the mean ± S.E. of three replicates. Statistical significance of differences between each treatment group and the control (**$p < 0.01$) or T090 without ajoene ($^{\#}p < 0.05$, $^{\#\#}p < 0.01$) was determined. Ajo, ajoene.

and obesity (25). Steatosis in the development of NAFLD is a strong risk factor for insulin resistance mostly observed in obese people. Overproduction and deposition of fat in hepatocytes is the primary event that stimulates progression of metabolic liver diseases (3). Moreover, it may progress to advanced liver diseases with associated morbidity and mortality: steatohepatitis and more severely to fibrosis, cirrhosis, and hepatocellular carcinoma (35). The present study was designed to determine the effects of ajoene on lipogenesis and hepatic steatosis using both an *in vivo* model involving mice fed an HFD and an *in vitro* model using a treatment of LXRα ligand on hepatocytes.

Since HFD feeding accompanies obesity and insulin resistance in animals, inducing fatty liver, the pathophysiologic features in animals are analogous to clinical metabolic diseases. Although rodents fed a methionine- and choline-deficient diet develop hepatic steatosis with inflammation, this diet feeding causes loss of body weight gain (e.g., muscle and fat) and does not develop insulin resistance (35). The period of HFD feeding and the amount of fat in the diet affect the metabolic phenotypes and liver histology. Usually, 40%–60% HFD feeding (% calories from fat) are used; body weight and plasma glucose level were both higher in 58% HFD-fed mice already after the first week (51), and liver fat levels increased within a week by this diet feeding (41). Indeed, our observation proved obvious fat accumulation in the liver after feeding of mice with 60% HFD for 8 weeks, which was evidenced by increases in Oil Red O staining and hepatic TG content. These phenotypic alterations were clearly antagonized by ajoene treatment (10 or 30 mg/kg/day) for the final 4 weeks of the HFD feeding. Moreover, ajoene significantly reduced the increased plasma TG and cholesterol levels, which is in line with the report that it inhibits cholesterol synthesis in hepatocytes (14, 43).

In addition, increased body weight gain in HFD-fed mice was diminished by treatment of 30 mg/kg/day ajoene. Although a low dose (10 mg/kg/day) of ajoene treatment non-significantly affected body weight gain, there was a trend to decrease it. So, successful inhibition of hepatic lipid accumulation by 10 mg/kg/day of ajoene treatment may be associated in part with anti-obesity action. Body weight gain is affected by the balance between energy supplement and consumption (26). Our data showing no change in the food intake after ajoene treatment suggest the possibility that ajoene has an effect on energy expenditure process. Interestingly, ajoene inhibits differentiation of preadipocytes and also induces adipocyte apoptosis (38, 53), which may account for its anti-obesity effect. Ajoene may also change dietary lipid absorption, as suggested by the finding that it inhibited human gastric lipase *in vitro* (13). Moreover, ajoene treatment

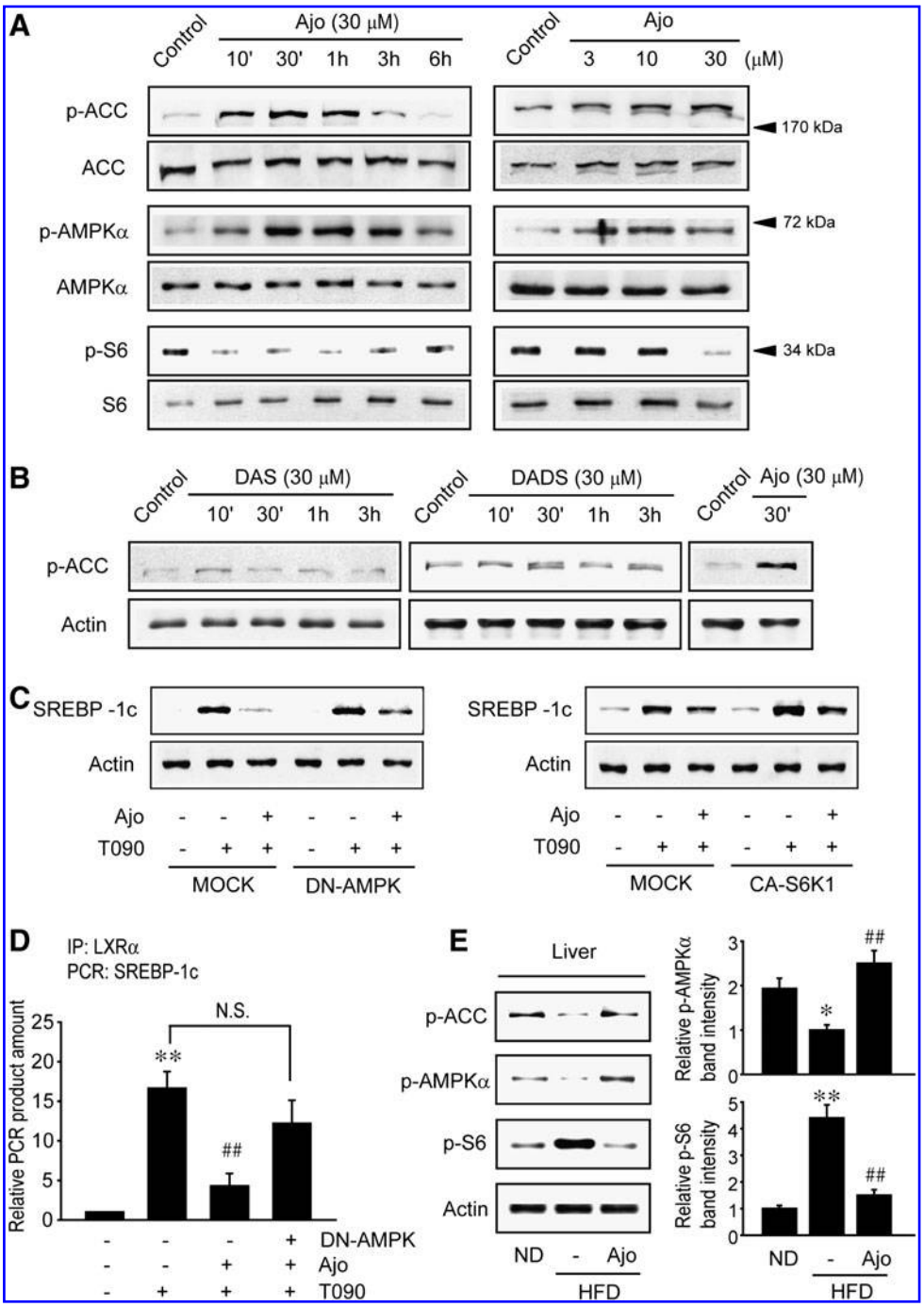

FIG. 8. The ability of ajoene to activate AMPK that leads to S6K1 inhibition. (**A**) AMPK activation and inhibition of S6 phosphorylation. Immunoblots were performed on the lysates of HepG2 cells that had been treated with ajoene (30 μM) for the indicated time period or different concentration of ajoene (3–30 μM) for 30 min. (**B**) The effects of DAS and DADS on ACC phosphorylation. Immunoblots were performed on the lysates of HepG2 cells that had been treated with either DAS or DADS (30 μM each) for the indicated time period. (**C**) The roles of AMPK and S6K1 in the ability of ajoene to inhibit SREBP-1c induction by T090. Immunoblots were performed on the lysates of HepG2 cells that had been treated with T090 or T090+ ajoene for 12 h following DN-AMPK or CA-S6K1 transfection. (**D**) ChIP assays. DNA–protein complexes were prepared from cells that had been treated with T090 or T090+ajoene for 6 h following DN-AMPK transfection, and were immunoprecipitated with anti-LXRα antibody or preimmune-IgG. The samples were subjected to PCR-amplification using DNA primers flanking the LXRE of SREBP-1c gene promoter. (**E**) Immunoblottings for phosphorylated ACC, AMPK, and S6. Proteins of interest were immunoblotted in the liver homogenates of ND-fed or HFD-fed mice that had been treated with vehicle or ajoene (30 mg/kg/day). Data represent the mean ± S.E. of three replicates. Statistical significance of differences between each treatment group and the control ($^{*}p < 0.05$, $^{**}p < 0.01$) or T090 without ajoene ($^{\#\#}p < 0.01$) was determined. Ajo, ajoene.

improved hyperglycemia and hyperinsulinemia induced by HFD feeding. Taken together, our results demonstrate that ajoene has the ability to inhibit hepatic steatosis, decrease body weight gain, and improve glucose metabolism.

Lipid-induced toxicity caused by fat overload may cause steatohepatitis (i.e., liver injury), which is a crucial step for progression to end-stage liver disease (35). Excessive oxidation of accumulated fatty acids generates large amounts of reactive oxygen species (ROS) in hepatocytes. Thus, oxidative stress is one of the key stimuli that mediate lipotoxic events and evoke pathologic development (34, 35); the radical stress triggers further production of lipid peroxides that make adducts to macromolecules, resulting in chronic damage to organelles such as mitochondria (35). The degeneration and apoptosis of parenchymal cells may lead to collapse of organ function. Moreover, oxidative stress stimulates the release of

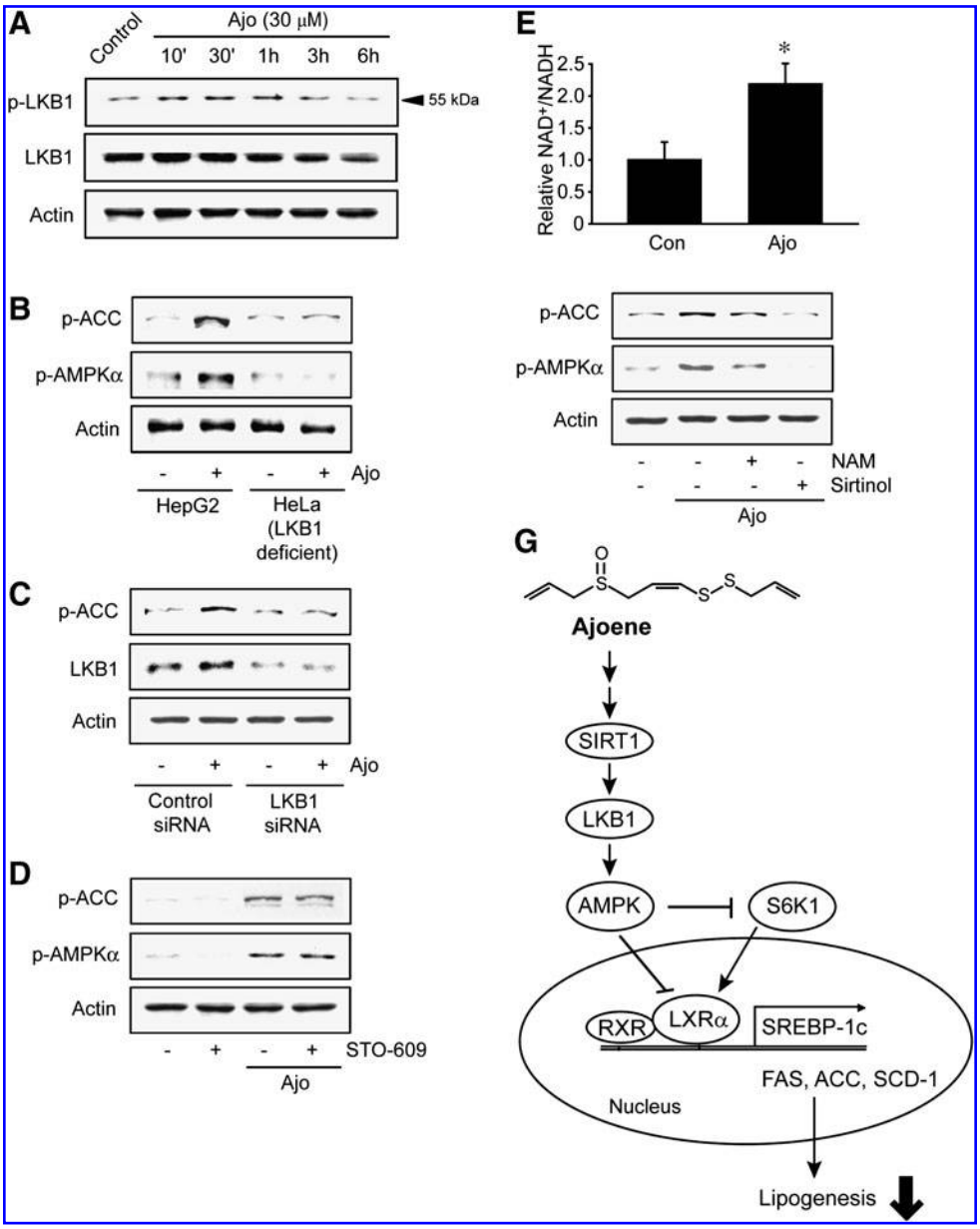

FIG. 9. LKB1-dependent AMPK activation by ajoene. (**A**) LKB1 phosphorylation. Immunoblots were performed on the lysates of HepG2 cells that had been treated with 30 μM ajoene for the indicated times. (**B**) AMPK activation. Hela cells deficient in LKB1 were treated with vehicle or ajoene for 1 h and subjected to immunoblot assay. (**C**) Effect of LKB1 siRNA knockdown. HepG2 cells were treated with ajoene for 1 h after siRNA transfection. (**D**) Effect of CaMKKβ inhibitor on the activation of AMPK. HepG2 cells were treated with 1 μg/ml STO-609 for 30 min, and continuously incubated with ajoene for 1 h. (**E**) Cellular NAD^+/NADH ratio. The contents of NAD^+ and NADH were measured in cells treated with 30 μM ajoene for 30 min. (**F**) Effects of SIRT1 inhibitors on the activation of AMPK by ajoene. HepG2 cells were treated with 10 mM nicotinamide (NAM) or 10 μM sirtinol for 30 min, and continuously incubated with ajoene for 1 h. (**G**) A schematic diagram illustrating the proposed mechanism by which ajoene inhibits LXRα-mediated hepatic steatosis. Ajo, ajoene.

inflammatory mediators. Imbalance of redox state and chronic inflammatory condition alter intracellular signaling, and thus impair energy metabolism (22, 50). Therefore, oxidative stress is critical for the development of NAFLD. In this study, HFD feeding indeed promoted oxidative stress, as shown by increases in TBARS and nitrotyrosinylation (i.e., ROS and RNS) with a decrease in cellular GSH content that was accompanied by hepatocytes injury (e.g., liver histopathology, inflammatory gene induction, and plasma ALT activity). Intriguingly, ajoene treatment reversed these pathologic changes: reduction of free radical stress and inflammatory response to damage. Our findings showed that ajoene attenuates steatohepatitis induced by fat accumulation, and that the beneficial effect may be associated with its inhibitory action on oxidative stress.

Garlic has been used as a remedy for disease as well as a food ingredient. The favorable actions of garlic are elicited mostly by diverse organosulfur components (15, 19). In particular, ajoene as one of organosulfur by-products derived from garlic has beneficial effects and chemical stability. Along with numerous studies of garlic on atherosclerosis and cancer, the hepatoprotective effect of garlic against toxicants has been also recognized (9, 10, 31). Our results shown here demonstrate for the first time that ajoene treats fatty liver and fat-induced oxidative stress, and which results mainly from the inhibition of lipogenesis.

A line of evidence indicates that abnormal hepatic fat accumulation in NAFLD patients results largely from *de novo* lipogenesis (8, 45). LXRα is highly expressed in liver, acting as a lipid sensing nuclear receptor to induce fat synthesis mainly through transcription of SREBP-1c, a master regulator of lipogenic genes (39). The lipogenic enzymes including FAS, ACC, and SCD-1 (i.e., targets of SREBP-1c) are involved in multiple steps of TG anabolic processes (3). The importance of LXRα in steatosis was proven by the findings that administration of LXR activator to mice induces hepatic lipogenesis

and TG accumulation, whereas a deficiency of LXR abolished this effect (42). Consistently, HFD feeding increased hepatic and plasma TG levels in mice, whereas no increase was found in LXR-null mice (21). In the present study, ajoene efficaciously antagonized LXRα and SREBP-1c gene expressions induced by HFD feeding in the liver tissue of mice, as further supported by the repression of lipogenic genes, FAS, ACC, and SCD-1.

Consistent with the results of an *in vivo* experimental model, ajoene inhibited LXRα agonist-induced SREBP-1c activation and lipogenic gene induction in hepatocytes, as shown by the results of immunoblot, real-time PCR, and reporter gene assays. The activity of LXRα is post-translationally controlled by phosphorylation. Recently, Hwahng *et al*. showed that AMPK and S6K1 oppositely regulate LXRα activity: the inhibitory and activating phosphorylations of LXRα are mediated by AMPK and S6K1, respectively (18). In the present study, the inhibitory effect of ajoene on LXRα induction of SREBP-1c was reversed by either AMPK inhibition or S6K1 activation, indicating that the antilipogenic effect may stem from LXRα inhibition as a consequence of AMPK activation that leads to S6K1 inhibition. Other kinases that modulate the activity of LXRα include protein kinase A and casein kinase-2 (47, 52). The effects of ajoene on these remain to be explored.

In addition to the antilipogenic effect of AMPK, it also regulates cellular lipid metabolism in large part through stimulation of fatty acid oxidation (48). We found that ajoene treatment increased the level of hepatic CPT-1, which is a downstream effecter of peroxisome proliferator-activated receptor (PPAR)-α [HFD alone, 1.00 ± 0.08; HFD+Ajo 10 mg/kg/day, 1.45 ± 0.16*; and HFD+Ajo 30 mg/kg/day, 1.83 ± 0.16** (statistical significance of difference from HFD, $^{*}p < 0.05$, $^{**}p < 0.01$)]. AMPK has also been shown to be involved in the control of mitochondrial biogenesis and adaptive mitochondrial function (40). In mice fed on an HFD, ajoene increased the level of hepatic PPARγ coactivator-1α (PGC-1α) mRNA [ND, 1.00 ± 0.16; HFD alone, 0.45 ± 0.04**; and HFD+Ajo 10 mg/kg/day, $0.64 \pm 0.06^{\#}$ (statistical significance of difference from ND, $^{**}p < 0.01$ or HFD alone, $^{\#}p < 0.05$)], suggesting that the activated AMPK upregulates PGC-1α and promotes mitochondrial biogenesis. Collectively, our results indicate that ajoene may have an additional effect to increase fatty acid oxidation in the liver.

AMPK activation exerts beneficial effects such as antisteatosis and antidiabetes, which may also be caused by its inhibition of S6K1 (2, 18). In the present study, phosphorylations of AMPK and ACC were both increased by ajoene treatment in hepatocytes with a compatible decrease in S6K1 activity; moreover, ajoene was more efficacious than other organosulfurs (i.e., DAS and DADS). Therefore this study identified ajoene as a component that regulates AMPK-S6K1 pathway and thereby represses LXRα activity. Other AMPK activators (e.g., dithiolethione and sauchinone) have an antisteatotic effect as well, which is mediated by the inhibition of LXRα (18, 28). LXRα may have a favorable effect on cholesterol and glucose metabolism (32). So it cannot be excluded that the beneficial effect of ajoene on plasma cholesterol, glucose, and insulin results from the AMPK regulation of other cascades apart from LXRα inhibition.

In the present study, ajoene activated AMPK through LKB1, but not CaMKK, implying that LKB1 may serve as an upstream kinase of AMPK activation elicited by ajoene. Emerging evidence supports that SIRT1, an NAD-dependent deacetylase, collaborates with AMPK to regulate energy metabolism (16). Our results showing an increase in NAD^{+}/NADH by ajoene and inhibition of ajoene-induced AMPK activation by SIRT1 inhibitors support the concept that SIRT1 is necessary for the LKB1-dependent activation of AMPK by ajoene. In addition, AMPK induces small heterodimer partner (SHP) by activating upstream stimulatory factor-1 (5); SHP then inhibits the SREBP-1c lipogenic pathway through LXRα inhibition (49). In a supplemental experiment, ajoene increased SHP mRNA level (~1.6-fold), supporting the possible role of SHP in the action of ajoene. Moreover, AMPK has the ability to protect mitochondria from oxidative stress in association with glycogen synthase kinase-3β phosphorylation (6).

Pharmacological interventions may achieve the therapeutic effects to prevent and/or to treat steatosis and steatohepatitis. Although insulin sensitizers are favorably used in clinical situations, some drugs, including thiazolidinediones, stimulate weight gain, which is an unwanted effect in NAFLD patients (11). Various antioxidants including radical scavengers are used to treat or delay the progression of steatosis. In our study, we found no direct radical scavenging effect of ajoene, as assessed by an experiment using 1,1-diphenyl-2-picrylhydrazyl. So, it is likely that the antioxidant effect of ajoene results from its ability to activate AMPK. In addition, we recently reported that ajoene induces antioxidant genes via Nrf2 activation (24). Moreover, ajoene inhibits the induction of inflammatory genes in macrophages (7), and has antiplatelet and anti-atherosclerosis effects (1). All of these effects add value to the potential of ajoene for the treatment of steatosis and steatohepatitis. Our finding that ajoene inhibits fat-induced radical stress further strengthens its potential application for steatohepatitis. Easy synthesis and chemical stability are also merits of this compound as a drug candidate.

Acknowledgments

This work was supported by the National Research Foundation of Korea grant funded by the Korea government (MEST)(No. 2010-0001706), Korea. CYH would like to thank the Seoul Science Fellowship program.

Author Disclosure Statement

No competing financial interests exist.

References

1. Apitz–Castro R, Badimon JJ, and Badimon L. Effect of ajoene, the major antiplatelet compound from garlic, on platelet thrombus formation. *Thromb Res* 68: 145–155, 1992.
2. Bae EJ, Yang YM, Kim JW, and Kim SG. Identification of a novel class of dithiolethiones that prevent hepatic insulin resistance via the adenosine monophosphate-activated protein kinase-p70 ribosomal S6 kinase-1 pathway. *Hepatology* 46: 730–739, 2007.
3. Browning JD and Horton JD. Molecular mediators of hepatic steatosis and liver injury. *J Clin Invest* 114: 147–152, 2004.
4. Buege JA and Aust SD. Microsomal lipid peroxidation. *Methods Enzymol* 52: 302–310, 1978.
5. Chanda D, Li T, Song KH, Kim YH, Sim J, Lee CH, Chiang JY, and Choi HS. Hepatocyte growth factor family nega-

tively regulates hepatic gluconeogenesis via induction of orphan nuclear receptor small heterodimer partner in primary hepatocytes. *J Biol Chem* 284: 28510–28521, 2009.
6. Choi SH, Kim YW, and Kim SG. AMPK-mediated GSK3beta inhibition by isoliquiritigenin contributes to protecting mitochondria against iron-catalyzed oxidative stress. *Biochem Pharmacol* 79: 1352–1362, 2010.
7. Dirsch VM, Kiemer AK, Wagner H, and Vollmar AM. Effect of allicin and ajoene, two compounds of garlic, on inducible nitric oxide synthase. *Atherosclerosis* 139: 333–339, 1998.
8. Donnelly KL, Smith CI, Schwarzenberg SJ, Jessurun J, Boldt MD, and Parks EJ. Sources of fatty acids stored in liver and secreted via lipoproteins in patients with nonalcoholic fatty liver disease. *J Clin Invest* 115: 1343–1351, 2005.
9. El–Beshbishy HA. Aqueous garlic extract attenuates hepatitis and oxidative stress induced by galactosamine/lipoploysaccharide in rats. *Phytother Res* 22: 1372–1379, 2008.
10. Flora SJ, Mehta A, and Gupta R. Prevention of arsenic-induced hepatic apoptosis by concomitant administration of garlic extracts in mice. *Chem Biol Interact* 177: 227–233, 2009.
11. Fonseca V. Effect of thiazolidinediones on body weight in patients with diabetes mellitus. *Am J Med* 115: 42S–48S, 2003.
12. Fujisawa H, Suma K, Origuchi K, Kumagai H, Seki T, and Ariga T. Biological and chemical stability of garlic-derived allicin. *J Agric Food Chem* 56: 4229–4235, 2008.
13. Gargouri Y, Moreau H, Jain MK, de Haas GH, and Verger R. Ajoene prevents fat digestion by human gastric lipase *in vitro*. *Biochim Biophys Acta* 1006: 137–139, 1989.
14. Gebhardt R, Beck H, and Wagner KG. Inhibition of cholesterol biosynthesis by allicin and ajoene in rat hepatocytes and HepG2 cells. *Biochim Biophys Acta* 1213: 57–62, 1994.
15. Hassan HT. Ajoene (natural garlic compound): A new anti-leukaemia agent for AML therapy. *Leuk Res* 28: 667–671, 2004.
16. Hou X, Xu S, Maitland-Toolan KA, Sato K, Jiang B, Ido Y, Lan F, Walsh K, Wierzbicki M, Verbeuren TJ, Cohen RA, and Zang M. SIRT1 regulates hepatocyte lipid metabolism through activating AMP-activated protein kinase. *J Biol Chem* 283: 20015–20026, 2008.
17. Hunter R, Kaschula CH, Parker IM, Caira MR, Richards P, Travis S, Taute F, and Qwebani T. Substituted ajoenes as novel anti-cancer agents. *Bioorg Med Chem Lett* 18: 5277–5279, 2008.
18. Hwahng SH, Ki SH, Bae EJ, Kim HE, and Kim SG. Role of adenosine monophosphate-activated protein kinase-p70 ribosomal S6 kinase-1 pathway in repression of liver X receptor-alpha-dependent lipogenic gene induction and hepatic steatosis by a novel class of dithiolethiones. *Hepatology* 49: 1913–1925, 2009.
19. Iciek M, Kwiecień I, and Włodek L. Biological properties of garlic and garlic-derived organosulfur compounds. *Environ Mol Mutagen* 50: 247–265, 2009.
20. Inoki K, Zhu T, and Guan KL. TSC2 mediates cellular energy response to control cell growth and survival. *Cell* 115: 577–590, 2003.
21. Kalaany NY, Gauthier KC, Zavacki AM, Mammen PP, Kitazume T, Peterson JA, Horton JD, Garry DJ, Bianco AC, and Mangelsdorf DJ. LXRs regulate the balance between fat storage and oxidation. *Cell Metab* 1: 231–244, 2005.
22. Kaneto H, Katakami N, Kawamori D, Miyatsuka T, Sakamoto K, Matsuoka TA, Matsuhisa M, and Yamasaki Y. Involvement of oxidative stress in the pathogenesis of diabetes. *Antioxid Redox Signal* 9: 355–366, 2007.
23. Kang KW, Kim YG, Cho MK, Bae SK, Kim CW, Lee MG, and Kim SG. Oltipraz regenerates cirrhotic liver through CCAAT/enhancer binding protein-mediated stellate cell inactivation. *FASEB J* 16: 1988–1990, 2002.
24. Kay HY, Yang JW, Kim TH, Lee DY, Kang B, Ryu JH, Jeon R, and Kim SG. Ajoene, a stable garlic by-product, has an antioxidant effect through Nrf2-mediated glutamate-cysteine ligase induction in HepG2 cells and primary hepatocytes. *J Nutr* 140: 1211–1219, 2010.
25. Kotronen A and Yki–Järvinen H. Fatty liver: A novel component of the metabolic syndrome. *Arterioscler Thromb Vasc Biol* 28: 27-38, 2008.
26. Kim MS, Park JY, Namkoong C, Jang PG, Ryu JW, Song HS, Yun JY, Namgoong IS, Ha J, Park IS, Lee IK, Viollet B, Youn JH, Lee HK, and Lee KU. Anti-obesity effects of alpha-lipoic acid mediated by suppression of hypothalamic AMP-activated protein kinase. *Nat Med* 10: 727–733, 2004.
27. Kim YW, Kang HE, Lee MG, Hwang SJ, Kim SC, Lee CH, and Kim SG. Liquiritigenin, a flavonoid aglycone from licorice, has a choleretic effect and the ability to induce hepatic transporters and phase-II enzymes. *Am J Physiol Gastrointest Liver Physiol* 296: G372–381, 2009.
28. Kim YW, Kim YM, Yang YM, Kim TH, Hwang SJ, Lee JR, Kim SC, and Kim SG. Inhibition of SREBP-1c-mediated hepatic steatosis and oxidative stress by sauchinone, an AMPK-activating lignan in *Saururus chinensis*. *Free Radic Biol Med* 48: 567–578, 2010.
29. Laffitte BA, Joseph SB, Walczak R, Pei L, Wilpitz DC, Collins JL, and Tontonoz P. Autoregulation of the human liver X receptor alpha promoter. *Mol Cell Biol* 21: 7558–7568, 2001.
30. Lage R, Diéguez C, Vidal–Puig A, and López M. AMPK: A metabolic gauge regulating whole-body energy homeostasis. *Trends Mol Med* 14: 539–549, 2008.
31. Lee SC, Hwang SY, Kim SW, and Kim SK. Ethanol extract of *Allium sativum* attenuates testicular and liver toxicity induced by 2,3,7,8-tetrachlorodibenzo-p-dioxin in rats. *J Med Food* 12: 93–99, 2009.
32. Lehrke M, Lebherz C, Millington SC, Guan HP, Millar J, Rader DJ, Wilson JM, and Lazar MA. Diet-dependent cardiovascular lipid metabolism controlled by hepatic LXRalpha. *Cell Metab* 1: 297–308, 2005.
33. Liang G, Yang J, Horton JD, Hammer RE, Goldstein JL, and Brown MS. Diminished hepatic response to fasting/refeeding and liver X receptor agonists in mice with selective deficiency of sterol regulatory element-binding protein-1c. *J Biol Chem* 277: 9520–9528, 2002.
34. Mantena SK, King AL, Andringa KK, Eccleston HB, and Bailey SM. Mitochondrial dysfunction and oxidative stress in the pathogenesis of alcohol- and obesity-induced fatty liver diseases. *Free Radic Biol Med* 44: 1259–1272, 2008.
35. Marra F, Gastaldelli A, Svegliati Baroni G, Tell G, and Tiribelli C. Molecular basis and mechanisms of progression of non-alcoholic steatohepatitis. *Trends Mol Med* 14: 72–81, 2008.
36. Meister A. Glutathione metabolism and its selective modification. *J Biol Chem* 263: 17205–17208, 1988.
37. Naganawa R, Iwata N, Ishikawa K, Fukuda H, Fujino T, and Suzuki A. Inhibition of microbial growth by ajoene, a sulfur-containing compound derived from garlic. *Appl Environ Microbiol* 62: 4238–4242, 1996.
38. Nelson–Dooley C, Della–Fera MA, Hamrick M, and Baile CA. Novel treatments for obesity and osteoporosis: Targeting apoptotic pathways in adipocytes. *Curr Med Chem* 12: 2215–2225, 2005.

39. Repa JJ, Liang G, Ou J, Bashmakov Y, Lobaccaro JM, Shimomura I, Shan B, Brown MS, Goldstein JL, and Mangelsdorf DJ. Regulation of mouse sterol regulatory element-binding protein-1c gene (SREBP-1c) by oxysterol receptors, LXRalpha and LXRbeta. *Genes Dev* 14: 2819–2830, 2000.
40. Reznick RM and Shulman GI. The role of AMP-activated protein kinase in mitochondrial biogenesis. *J Physiol* 574: 33–39, 2006.
41. Samuel VT, Liu ZX, Qu X, Elder BD, Bilz S, Befroy D, Romanelli AJ, and Shulman GI. Mechanism of hepatic insulin resistance in non-alcoholic fatty liver disease. *J Biol Chem* 279: 32345–32353, 2004.
42. Schultz JR, Tu H, Luk A, Repa JJ, Medina JC, Li L, Schwendner S, Wang S, Thoolen M, Mangelsdorf DJ, Lustig KD, and Shan B. Role of LXRs in control of lipogenesis. *Genes Dev* 14: 2831–2838, 2000.
43. Sendl A, Schliack M, Löser R, Stanislaus F, and Wagner H. Inhibition of cholesterol synthesis *in vitro* by extracts and isolated compounds prepared from garlic and wild garlic. *Atherosclerosis* 94: 79–85, 1992.
44. Stadler K, Bonini MG, Dallas S, Jiang J, Radi R, Mason RP, and Kadiiska MB. Involvement of inducible nitric oxide synthase in hydroxyl radical-mediated lipid peroxidation in streptozotocin-induced diabetes. *Free Radic Biol Med* 45: 866–874, 2008.
45. Tamura S and Shimomura I. Contribution of adipose tissue and de novo lipogenesis to nonalcoholic fatty liver disease. *J Clin Invest* 115: 1139–1142, 2005.
46. Taylor P, Noriega R, Farah C, Abad MJ, Arsenak M, and Apitz R. Ajoene inhibits both primary tumor growth and metastasis of B16/BL6 melanoma cells in C57BL/6 mice. *Cancer Lett* 239: 298–304, 2006.
47. Torra IP, Ismaili N, Feig JE, Xu CF, Cavasotto C, Pancratov R, Rogatsky I, Neubert TA, Fisher EA, and Garabedian MJ. Phosphorylation of liver X receptor alpha selectively regulates target gene expression in macrophages. *Mol Cell Biol* 28: 2626–2636, 2008.
48. Viollet B, Mounier R, Leclerc J, Yazigi A, Foretz M, and Andreelli F. Targeting AMP-activated protein kinase as a novel therapeutic approach for the treatment of metabolic disorders. *Diabetes Metab* 33: 395–402, 2007.
49. Watanabe M, Houten SM, Wang L, Moschetta A, Mangelsdorf DJ, Heyman RA, Moore DD, and Auwerx J. Bile acids lower triglyceride levels via a pathway involving FXR, SHP, and SREBP-1c. *J Clin Invest* 113: 1408–1418, 2004.
50. Wellen KE and Hotamisligil GS. Inflammation, stress, and diabetes. *J Clin Invest* 115: 1111–1119, 2005.
51. Winzell MS and Ahrén B. The high-fat diet-fed mouse: A model for studying mechanisms and treatment of impaired glucose tolerance and type 2 diabetes. *Diabetes* 53 Suppl 3: S215–S219, 2004.
52. Yamamoto T, Shimano H, Inoue N, Nakagawa Y, Matsuzaka T, Takahashi A, Yahagi N, Sone H, Suzuki H, Toyoshima H, and Yamada N. Protein kinase A suppresses sterol regulatory element-binding protein-1C expression via phosphorylation of liver X receptor in the liver. *J Biol Chem* 282: 11687–11695, 2007.
53. Yang JY, Della–Fera MA, Hausman DB, and Baile CA. Enhancement of ajoene-induced apoptosis by conjugated linoleic acid in 3T3-L1 adipocytes. *Apoptosis* 12: 1117–1128, 2007.

Address correspondence to:
Sang Geon Kim, Ph.D.
College of Pharmacy
and Research Institute of Pharmaceutical Sciences
Seoul National University
Sillim-dong, Kwanak-gu
Seoul 151-742
Korea

E-mail: sgk@snu.ac.kr

Date of first submission to ARS Central, March 17, 2010; date of final revised submission, May 27, 2010; date of acceptance, June 19, 2010.

Abbreviations Used

ACC = acetyl-CoA carboxylase
ALT = alanine aminotransferase
AMPK = AMP-activated protein kinase
CA = constitutively active
CaMKK = calcium/calmodulin-dependent kinase kinase
COX-2 = cyclooxygenase-2
CPT-1 = carnitine palmitoyl transferase-1
DADS = diallyl disulfide
DAS = diallyl sulfide
DN = dominant negative
FAS = fatty acid synthase
GPx = glutathione peroxidase
HFD = high-fat diet
iNOS = inducible nitric oxide synthase
LKB1 = liver kinase B1
LXRα = liver X receptor-α
LXRE = LXR response element
m-CPBA = meta-chloroperoxybenzoic acid
NAFLD = nonalcoholic fatty liver disease
ND = normal diet
PGC-1α = PPARγ coactivator-1α
PPAR = peroxisome proliferator-activated receptor
RNS = reactive nitrogen species
ROS = reactive oxygen species
SCD = stearoyl-CoA desaturase
SHP = small heterodimer partner
SIRT1 = silent information regulator T1
SREBP-1c = sterol regulatory element binding protein-1c
T090 = T0901317
TBARS = thiobarbituric acid reactive substances
TG = triglyceride

This article has been cited by:

1. Zi-Feng Zhang, Jun Lu, Yuan-Lin Zheng, Dong-Mei Wu, Bin Hu, Qun Shan, Wei Cheng, Meng-Qiu Li, Yuan-Yuan Sun. 2012. Purple sweet potato color attenuates hepatic insulin resistance via blocking oxidative stress and endoplasmic reticulum stress in high-fat-diet-treated mice. *The Journal of Nutritional Biochemistry* . [CrossRef]
2. Hee Yeon Kay , Won Dong Kim , Se Jin Hwang , Hueng-Sik Choi , Richard K. Gilroy , Yu-Jui Yvonne Wan , Sang Geon Kim . 2011. Nrf2 Inhibits LXR#-Dependent Hepatic Lipogenesis by Competing with FXR for Acetylase Binding. *Antioxidants & Redox Signaling* **15**:8, 2135-2146. [Abstract] [Full Text HTML] [Full Text PDF] [Full Text PDF with Links] [Supplemental material]
3. Wei Zhu, Qianju Jia, Yun Wang, Yuhua Zhang, Min Xia. 2011. The anthocyanin cyanidin-3-O-#-glucoside, a flavonoid, increases hepatic glutathione synthesis and protects hepatocytes against reactive oxygen species during hyperglycemia: Involvement of a cAMP–PKA-dependent signaling pathway. *Free Radical Biology and Medicine* . [CrossRef]